symmetry

IMPACT FACTOR 2.2

CITESCORE 5.4

Article

Bound States and Particle Production by Breather-Type Background Field Configurations

Abhishek Rout and Brett Altschul

MDPI

https://doi.org/10.3390/sym16121571

symmetry

MDPI

Article

Bound States and Particle Production by Breather-Type Background Field Configurations

Abhishek Rout and Brett Altschul *

Department of Physics and Astronomy, University of South Carolina, Columbia, SC 29208, USA; arout@email.sc.edu
* Correspondence: altschul@mailbox.sc.edu

Abstract: We investigate the interaction of fermion fields with oscillating domain walls, inspired by breather-type solutions of the sine-Gordon equation, a nonlinear system of fundamental importance. Our study focuses on the fermionic bound states and particle production induced by a time-dependent scalar background field. The fermions couple to two domain walls undergoing harmonic motion, and we explore the resulting dynamics of the fermionic wave functions. We demonstrate that while fermions initially form bound states around the domain walls, the energy provided by the oscillatory motion of the scalar field induces an outward flux of fermions and antifermions, leading to particle production and eventual flux propagation toward spatial infinity. Through numerical simulations, we observe that the fermion density exhibits quasiperiodic behavior, with partial recurrences of the bound state configurations after each oscillation period. However, the fermion wave functions do not remain localized, and over time, the density decreases as more particles escape the vicinity of the domain walls. Our results highlight that the sine-Gordon-like breather background, when coupled non-supersymmetrically to fermions, does not preserve integrability or stability, with the oscillations driving a continuous energy transfer into the fermionic modes. This study sheds light on the challenges of maintaining steady-state fermion solutions in time-dependent topological backgrounds and offers insights into particle production mechanisms in nonlinear dynamical systems with oscillating solitons.

Keywords: sine-Gordon equation; breather solitons; Jackiw-Rebbi fermions; non-integrable systems; fermion-antifermion flux

Citation: Rout, A.; Altschul, B. Bound States and Particle Production by Breather-Type Background Field Configurations. *Symmetry* **2024**, *16*, 1571. https://doi.org/10.3390/sym16121571

Academic Editors: Jorge Segovia and Ignatios Antoniadis

Received: 11 October 2024
Revised: 6 November 2024
Accepted: 20 November 2024
Published: 24 November 2024

1. Introduction

Particle production by extended classical structures is a topic that has been studied since the earliest days of quantum mechanics. In nontrivial spacetime backgrounds, this has been an incredibly fruitful line of inquiry, with the theoretical discoveries of the Unruh effect (for an accelerating observer) [1] and Hawking radiation (in a black hole spacetime) [2] having fundamentally changed our understanding of spacetime physics. The creation of particles can be seen as a process of transitions between different Fock states of a quantum theory embedded in an interesting classical background, and the relevant background can involve fields other than the spacetime metric. In particular, the coupling of quantum-mechanical particles to classical scalar and vector fields can have many intriguing consequences [3–9]. The nonlinear interactions responsible for both the shapes of solitary waves and the effective couplings between multiple solitary waves [10–15] are significant topics of research by themselves. For instance, during a sufficiently energetic collision of a solitary wave pair in $1+1$ dimensions, there may be a strongly inelastic bounce—in which one or both of the solitary waves rebound from the impact with internal modes or continuum scalar field modes excited. Over long times, the behavior of repeatedly colliding and rebounding solitary waves may display an intricate "fractal" dependence on the initial conditions [16–21].

However, when the background involves an extended structure built out of a bosonic field, the coupling of one or more additional fermion fields can be considered particularly interesting. Even without particle creation, the coupling of fermions to a topologically nontrivial bosonic field configuration can lead to the fascinating phenomenon of fermion fractionalization [3]. The nontrivial topology of the background may produce a potential for the fermion field whose spectrum is guaranteed to include a nondegenerate zero mode. When the fermion field is quantized, with the Dirac sea of negative-energy states filled, the zero mode is assigned partially to the Dirac sea and partially to the positive-energy part of the spectrum. The level in the energy spectrum at which the fermion number n_F vanishes actually lies in the middle of the zero mode [22]. Since the zero mode cannot ever actually be only partially filled, the real Fock states (with the mode filled or unfilled) consequently have non-integer values of n_F [23,24].

The situation may be even more complicated when there are multiple solitary wave structures present in the background. In the presence of multiple stationary solitons, there are typically multiple zero-energy (or almost-zero-energy) modes as part of the fermionic spectrum. When the solitary wave features are in motion relative to one another, this is further augmented by the possibility of fermion or antifermion particle creation [25], and it is a type of scenario like this that will be the focus of this paper. This is part of an ongoing research program [26], which has so far examined the fermion spectrum in backgrounds with two or three solitary waves. However, one of the challenges to doing calculations in a theory like this—in which the energy differences between fermion states bound to bosonic solitary wave may be exponentially small—is that the background may not be known precisely. Solitary waves are a feature of nonlinearly coupled classical fields, and in most cases analytic solutions involving multiple topological excitations are either unknown or extraordinarily complicated and impossible to express concisely. Small discrepancies between the precise energies of the background field configurations and the approximate forms used for calculational expediency may become a problem when trying to study the very small energy differences between neighboring fermion states.

In this paper, we shall look at fermion solutions in a particular type of background, inspired by the sine-Gordon equation in $1+1$ dimensions, since the sine-Gordon equation has time-dependent, multiple-soliton solutions that are known analytically. The focus will continue to be on the manifold of almost-zero-energy states that generalize the Jackiw–Rebbi zero modes; our work represents new fundamental advances in this area of investigation. In Section 2, we shall review the sine-Gordon equation and its breather-type soliton solutions. The consideration of a breather background was motivated by the hope that the breathers, which are bound soliton–antisoliton states with periodic time dependence, might support fermion bound states that were similarly periodic and for which analytic solutions might even be found. However, solving the Dirac equation in this kind of time-dependent background still turns out to be too difficult to achieve analytically, so in Section 3, we introduce another kind of bosonic background, inspired by the sine-Gordon breather but involving step functions that make the fermionic theory amenable to additional analytic solutions methods. In Section 4, we show, using a Fourier decomposition of the fermionic modes, that neither the step function background nor the true sine-Gordon breather background can actually have steady-state fermion solutions. There is an unavoidable outward flux in the fermion and antifermion nodes, driven energetically by the oscillations of the background scalar field. This is an entirely new result. In Section 5, we discuss the computational challenges this poses and present numerical results for how fermionic states that start off closely bound to the solitary waves in the background produce a wave of flux escaping to spatial infinity. Section 6 gives our final conclusions.

2. Breather Solitons

The sine-Gordon theory for a scalar field in $1+1$ dimensions has the Lagrange density

$$\mathcal{L}_\phi = \frac{1}{2}(\partial^\mu \phi)(\partial_\mu \phi) - \frac{1}{\pi}[1 - \cos(\pi\phi)]. \tag{1}$$

The theory this describes is extremely special, having degenerate vacua at all $\phi = n$ and solitary wave solutions that interpolate between them. These solitary waves are quite unusual, since they can pass through one another with no net deformations or radiation once they are well separated again. The solitary waves are thus actually "solitons" in the oldest and strongest sense of that term. The theory is integrable, a particularly unusual property in a relativistic theory and one that is closely connected to the solitary wave structure. The schematic (but nonrigorous) argument that the presence of true solitons means that there must be an infinite number of conservation laws is fairly straightforward. Suppose that N solitons are moving along the x-axis; any $N \geq 0$ is possible. They can all have different speeds, so that as $t \to \infty$, the separations between the solitary waves will become arbitrarily large, and thus the fraction of the total energy that remains tied up in the interactions between the solitons shrinks to an arbitrarily small amount. Each soliton is essentially an isolated system with conserved internal and kinetic energies of its own; and since N may be arbitrarily large, there must likewise be an unlimited number of these conservation laws. Such localized single-soliton energies are quite different from the usual way in which the infinite family of sine-Gordon conservation laws are normally expressed. However, the motivation for this argument was simply to show the deep connection between the existence of many-soliton solutions for ϕ and the existence of an infinite number of conservation laws. (Related analyses of integrable equations in $2+1$ dimensions are also currently an active area of study [27–30].)

A very natural question to ask is how many of the special properties of the sine-Gordon theory persist when the bosonic theory is coupled to a Dirac fermion field. Solutions with single solitary waves coupled to the fermions are well understood, with the unusual observation being the presence of zero-energy bound state modes and the surprising consequence that the fermion number actually has fractional eigenvalues [3]—among other anomalous features [31–34]. Studying fermions in scalar backgrounds composed of multiple solitary waves is a complicated subject, however. Normally, it is only amenable to approximate analyses—whether analytical or numerical [26,35–38]. However, one might hope that the simplicity of the sine-Gordon system would make it more straightforward to locate complete analytic solutions of the coupled boson–fermion system. Unfortunately, this does not seem to be the case, and, in fact, the first step in our analysis will be to replace the sine-Gordon breather background with a seemingly artificial approximation. Nonetheless, we shall find that our results can reveal quite a bit about the general structure of the Dirac theory in a time-dependent oscillatory topological background.

Beyond scattering states, in which two sine-Gordon solitons collide—either passing through each other or rebounding—there are also bound states of the solitons. In particular, the sine-Gordon equation has breather solutions (normalized so that they interpolate between vacuum states at $\phi = -1$, 0, and 1 and oscillate with period $2\pi\sqrt{1+b^2}/b$),

$$\phi_b(x,t) = \frac{4}{\pi}\tan^{-1}\left[\frac{\sin\left(bt/\sqrt{1+b^2}\right)}{b\cosh\left(x/\sqrt{1+b^2}\right)}\right]; \tag{2}$$

and the fermion Lagrange density in the presence of the sine-Gordon background field ϕ is

$$\mathcal{L}_\psi = \bar{\psi}\left[i\partial\!\!\!/ + g\cos\left(\frac{\pi}{2}\phi\right)\right]\psi. \tag{3}$$

This is the "natural" form for the coupling of the Dirac field to the scalar, because with a properly chosen value of g, the action becomes supersymmetric. In that case, the interactions in the boson and fermion Lagrange densities each descend from a "superpotential" $W(\phi) = \sin(\pi\phi/2)$, since $(1-\cos\pi\phi) \propto W^2$ and $\cos(\pi\phi/2) \propto dW/d\phi$. (However, ref. [37] used an ordinary Yukawa coupling even when the bosons obeyed a sine-Gordon equation.) Perhaps ironically, however, we do not actually expect our general conclusions to apply in the precisely supersymmetric sine-Gordon model, which remains integrable—like the

purely bosonic model [39,40]. The existence of an infinite number of degrees of freedom can qualitatively change the behavior of the system.

3. Dirac Equation in the Kink–Antikink Background

Unfortunately, no analytic solutions to the Dirac equation in the breather background have been forthcoming. So instead of the anharmonically oscillating sine-Gordon breather solution, we shall take two-step function domain walls undergoing simple harmonic motion back and forth through one another, with amplitude $v \geq 0$ and frequency ω,

$$\phi(x,t) = \mathrm{sgn}(x - v\cos\omega t) - \mathrm{sgn}(x + v\cos\omega t). \tag{4}$$

[We shall refer to the first term on the right-hand side of (4) as the "kink", which is located at positive x at the initial time $t = 0$, and the second term as the "antikink".] In this case, the scalar potential appearing in the Dirac equation $[i\partial\!\!\!/ + V(x,t)]\psi = 0$ is

$$V(x,t) = g\,\mathrm{sgn}\Big(x^2 - v^2\cos^2\omega t\Big), \tag{5}$$

so with the Dirac matrix representation $\gamma_0 = \sigma_1$ and $\gamma_1 = i\sigma_3$, the 2×2 matrix form of the Dirac equation becomes

$$\begin{bmatrix} \partial_x + g\,\mathrm{sgn}\big(x^2 - v^2\cos^2\omega t\big) & i\partial_t \\ i\partial_t & -\partial_x + g\,\mathrm{sgn}\big(x^2 - v^2\cos^2\omega t\big) \end{bmatrix} \begin{bmatrix} \psi_1 \\ \psi_2 \end{bmatrix} = \begin{bmatrix} 0 \\ 0 \end{bmatrix}. \tag{6}$$

With a Yukawa coupling $-g\phi\bar{\psi}\psi$ (as would be natural in a ϕ^4 theory) instead of the cosine coupling term in (3), a kink would produce an attractive potential for the upper component ψ_1 of the Dirac wave function, and repulsive potential for the lower component ψ_2. The zero-mode wave function for a bound fermion attached to a single stationary signum function located at x_K would be (assuming a coupling strength $g > 0$)

$$\begin{bmatrix} \psi_1 \\ \psi_2 \end{bmatrix} = \left[\frac{g4^g\Gamma(g+\frac{1}{2})}{\sqrt{\pi}\,\Gamma(g+1)}\right]^{1/2} \begin{bmatrix} e^{-g|x-x_K|} \\ 0 \end{bmatrix}. \tag{7}$$

Similarly, the zero mode attached to an isolated antikink has only its lower component nonzero. The specific exponential wave functions are particular to the infinitely narrow domain walls, but the general property that one component of the zero-mode wave function vanishes is generic, applying in any stationary background for which $V(-\infty)$ and $V(+\infty)$ have opposite signs.

In contrast, with interaction (3), what determines which component of a zero-mode wave function attached to a solitary wave is nonzero is not whether ϕ is increasing (kink) or decreasing (antikink). Instead, it depends on whether the cosine function in $\mathcal{L}_\psi$ is increasing or decreasing across the solitary wave. That is determined by whether a particular solitary wave interpolates from an even to an odd vacuum value—meaning from $V(-\infty) = 2n$ to $V(+\infty) = 2n \pm 1$—or from an odd vacuum to an even one. A kink interpolating between the degenerate vacua at $\phi = 0$ and $\phi = 1$ acts the same way on the Dirac wave function as an antikink interpolating between $\phi = 0$ and -1.

In the presence of a well-separated kink–antikink pair, there are two almost-zero-energy fermion modes, with even and odd behaviors under parity. When the domain walls are far apart, the corresponding fermion wave functions are well approximated by symmetric and antisymmetric linear combinations of a purely-ψ_1 bound state wave function tightly localized around one domain wall's location and a purely-ψ_2 function localized around the other solitary wave. In this regime, the two fermion states are approximately equally displaced above and below zero energy. In contrast, when the kink and antikink draw close together, so that $v|\cos\omega t| \lesssim g^{-1}$, the wave functions become much more complicated. Both ψ_1 and ψ_2 are appreciable in the neighborhood of $x = 0$, and their energy shifts are no longer equal and opposite. Moreover, even though the kink and

antikink pass through one another, the almost-zero-energy modes do not follow along. After their episodes of complicated mixing during each interval in which $v|\cos\omega t| \lesssim g^{-1}$, the ψ_1-dominated and ψ_2-dominated portions of the full wave function do not pass through each other but instead rebound, switching their locations of attachments from kink to antikink and vice versa. The wave function ψ is periodic with period π/ω, like V, rather than the $2\pi/\omega$ periodicity of ϕ itself. Moreover, the evolution of the system during the collision period cannot be adiabatic; although the adiabatic approximation may be excellent when the kink and antikink are widely separated, the field backgrounds (2) or (4) both pass through the state $\phi = 0$—which is a background in which the discrete modes of the instantaneous Hamiltonian merge into a massless continuum that extends through $E = 0$ with no gap.

Using a prime to denote a derivative with respect to x and a dot one with respect to t, the coupled partial differential Equation (6) for the upper and lower components are

$$\psi_1' + V\psi_1 + i\dot{\psi}_2 = 0; \tag{8}$$
$$-\psi_2' + V\psi_2 + i\dot{\psi}_1 = 0. \tag{9}$$

Unlike the system of time-independent energy eigenvalues, these cannot be fully separated, because of the time dependence of the potential V. From the general forms (8) and (9), we may differentiate (8) spatially and use the time derivative of (9) to eliminate $\dot{\psi}_2'$. However, since (9) involves both ψ_2' and ψ_2, this substitution introduces terms with a $V\dot{\psi}_2$ and $\dot{V}\psi_2$; the first of these may be eliminated in turn by one more substitution of the (undifferentiated) (8), but the second one, which appears because of the time dependence of V, cannot. This leaves the two equations still unavoidably coupled. The final resulting equations for both components of ψ are

$$\ddot{\psi}_1 - \psi_1'' + (V^2 - V')\psi_1 - i\dot{V}\psi_2 = 0; \tag{10}$$
$$\ddot{\psi}_2 - \psi_2'' + (V^2 + V')\psi_2 - i\dot{V}\psi_1 = 0. \tag{11}$$

For the particular $V(x,t) = g\,\mathrm{sgn}\left(x^2 - v^2\cos^2\omega t\right)$, this simplifies even further, since $V^2 = g^2$, so that except at the locations of the kink and antikink, each equation simply has the form of a free massive Klein–Gordon equation, $(\Box + g^2)\psi_j = 0$. Moreover, since $\dot{V} = -v\omega\sin(\omega t)V'$, we have

$$(\Box + g^2)\psi_j + (-1)^j 2g[\delta(x - v|\cos\omega t|) - \delta(x + v|\cos\omega t|)]\Big[\psi_j + (-1)^j iv\omega\sin(\omega t)\psi_{3-j}\Big] = 0. \tag{12}$$

The fact that the solitary wave located at positive $x = v|\cos\omega t|$ is always the one that is attractive to the ψ_1 component and repulsive to ψ_2, regardless of whether the solitary wave is a kink or antikink is again evident in this equation. Using a Klein–Gordon Green's function, these two coupled partial differential equations could be converted into two coupled double-integral equations; then, the δ-functions would eliminate one of the two integrations, although it is not clear whether this could be useful in practice.

4. Fourier Modes of the Dirac Equation

Since the potential V is periodic with period π/ω, any steady-state solution ought to be as well, so we can try representing ψ as a Fourier series,

$$\psi(x,t) = \sum_{n=-\infty}^{\infty} \begin{bmatrix} \psi_{1n}(x)e^{-2in\omega t} \\ \psi_{2n}(x)e^{-2in\omega t} \end{bmatrix}. \tag{13}$$

However, this does not, on its own, split up the Dirac equation into a set of linear ordinary differential equations for the ψ_{jn} Fourier components, because the left-hand side of (6) is

still time-dependent. However, we may also Fourier transform the step function V. For each x,

$$V(x,t) = g\left[\frac{1}{2}c_0(x) + \sum_{m=1}^{\infty} c_m(x)\cos(2m\omega t)\right], \tag{14}$$

so that, for $m \neq 0$,

$$\int_0^{\pi/\omega} dt\, g\,\mathrm{sgn}\left(x^2 - v^2\cos^2\omega t\right)\cos(2m\omega t) = g\sum_{m'=1}^{\infty} c_{m'}(x)\int_0^{\pi/\omega} dt\,\cos(2m'\omega t)\cos(2m\omega t), \tag{15}$$

in which the right-hand side is simply $(\pi g/2\omega)c_m(x)$. The signum function splits the left-hand side into two integrals,

$$g\int_0^{t_0} dt\,[-\cos(2m\omega t)] + g\int_{t_0}^{\pi/\omega} dt\,\cos(2m\omega t) = -\frac{2g}{2m\omega}\sin(2m\omega t_0), \tag{16}$$

where t_0 is the time at which the kink is located at position x,

$$t_0 = \begin{cases} 0, & |x| > v \\ \frac{1}{\omega}\cos^{-1}\frac{|x|}{v}, & |x| < v \end{cases}. \tag{17}$$

This makes the Fourier coefficients

$$c_{m>0}(x) = \begin{cases} 0, & |x| > v \\ -\frac{2}{m\pi}\sin\left(2m\cos^{-1}\frac{|x|}{v}\right), & |x| < v \end{cases}. \tag{18}$$

For the $m = 0$ case, the left-hand side of (16) is simply $g[(\pi/\omega) - 2t_0]$, and so $c_0(x)$, which is just twice the time average of V at the location x, is

$$c_0(x) = \begin{cases} 2, & |x| > v \\ 2\left(1 - \frac{4}{\pi}\cos^{-1}\frac{|x|}{v}\right), & |x| < v \end{cases}. \tag{19}$$

The fact that V is time-dependent means that all the spatial differential equations for the ψ_{jn} are coupled together, so solving the system is still a challenge. In fact, inserting the Fourier expansion of V into (8) and (9) produces an infinite number of coupled first-order linear differential equations. However, when $|x|$ is larger than the domain walls' oscillation amplitude v, then the signum function is 1 at all times (all $c_{m>0} = 0$), and the equations for the ψ_{jn} decouple,

$$\psi_{1n}' + g\psi_{1n} + 2n\omega\psi_{2n} = 0; \tag{20}$$

$$-\psi_{2n}' + g\psi_{2n} + 2n\omega\psi_{1n} = 0, \tag{21}$$

and have straightforward solutions,

$$\psi_{1n} = A_n e^{i\sqrt{4n^2\omega^2 - g^2}\,x} + B_n e^{-i\sqrt{4n^2\omega^2 - g^2}\,x} \tag{22}$$

$$\psi_{2n} = -A_n\frac{g + i\sqrt{4n^2\omega^2 - g^2}}{n\omega}e^{i\sqrt{4n^2\omega^2 - g^2}\,x} - B_n\frac{g - i\sqrt{4n^2\omega^2 - g^2}}{n\omega}e^{-i\sqrt{4n^2\omega^2 - g^2}\,x} \tag{23}$$

as complex exponentials. For large $|g| > 2|n|\omega$, these solutions look quite reasonable as Fourier components of a wave function; either A_n or B_n will vanish so that there is no exponential growth at infinity, and the asymptotic spatial behavior is $\psi_{jn} \sim e^{-\sqrt{g^2 - 4n^2\omega^2}\,|x|}$.

However, it may initially appear that things go awry for large $|n|$. It seems extremely unlikely that all the Fourier components will be identically zero for $|x| > v$ beyond some maximum $|n|$. Yet, if arbitrarily high-frequency terms are present in the Fourier expansion, then it is clear that beyond $|n| > |g|/2\omega$, the ψ_{jn} terms will not be exponentially decaying as $|x| \to \infty$, but will instead exhibit spatial oscillations.

The resolution to this puzzle comes from the fact that the Dirac wave function does not have a true single-particle probabilistic interpretation and need not be normalizable. There is the well-known Klein paradox [41,42], in which a repulsive external potential of height greater than $2m$ can have oscillatory solutions where the potential is highest. In that situation, the potential can supply enough energy to create real fermion–antifermion pairs, and the presence of oscillatory solutions in the classical forbidden region is a manifestation of this effect. In the situation we are examining here, there is likewise an external source of energy that may be transferred to the fermion field via particle creation. Regardless of how small g and v are, the back-and-forth oscillations of the domain wall pair can eventually contribute enough energy to create real outgoing particles, because the oscillations have been taken to continue eternally. Over time, it is possible for the Dirac field to absorb $|n|$ quanta from the coherent domain wall oscillations, regardless of how large $|n|$ is.

So the solutions of the Dirac equation in the time-dependent background cannot be expected to show only exponential damping at large $|x|$; there is also the possibility of an outflow of particles. For a mode to have enough energy to represent escaping continuum particles, it needs to represent the transfer of enough quanta of energy ω to create the massive particles that escape to infinity; but these are precisely the modes for which $\sqrt{4n^2\omega^2 - g^2}$ is real! Setting boundary conditions so that there are only outgoing quanta (no incoming modes excited) and including the time dependences of the components, the long-range behavior is

$$\psi_{jn} e^{-2in\omega t} \sim e^{2in\omega\left(\sqrt{1-g^2/4n^2\omega^2}\,|x|-t\right)}. \tag{24}$$

The observation that a steady-state, (π/ω)-periodic solution of the Dirac equation necessarily involves an outgoing flux of quanta from the kink–antikink region suggests that the one of the original reasons for focusing especially on the sine-Gordon breather system was misguided. The purely bosonic sine-Gordon theory is integrable, with an infinite number of conserved quantities. Recall that the solitary waves are true "solitons" in the strong sense, in that while they exert net forces on one another, when they collide, they pass through one another and, as they separate to great distances, return to their original shapes. In particular, while there are the breather solutions, in which a kink and an antikink form a bound state, never will a kink and an antikink annihilate into non-topological low-amplitude radiation excitations. It was hoped that including appropriately coupled fermions in the theory (perhaps in the version of the boson–fermion theory which differs from the supersymmetric theory only in the magnitude of the coupling constant) might preserve the integrability of the theory and the absolute stability of individual solitary waves. However, the argument for the structure (24) for the large-n Fourier modes' behavior in the far field does not depend in any fundamental way on the specific step function approximation for the ϕ background; the reasoning would apply equally well with (2) as with (4). Any one of the large-n modes should generally be excited, unless there is a conservation law that prohibits such an excitation. This is why the choice of coupling that makes the fermion-coupled sine-Gordon model truly supersymmetric differs from all other values. The supersymmetric version has an infinite number of conservation laws and is thus capable of preventing the excitation of the infinite number of outward-propagating modes and preserving perpetual breathers. However, the fact that the solutions of the Dirac equation in a breather-like background otherwise involve outward net flux suggests that any hope that the most general sine-Gordon theory coupled to fermions might remain fully integrable appears to be untenable.

5. Computational Complications and Results

The fact that fermionic modes can propagate outside the kink–antikink region (completely freely in the square wave model, nearly freely in the more realistic sine-Gordon theory) poses numerical as well as analytical challenges. Because of the greater complexity of the sine-Gordon breather system, we shall continue to focus, as we move to numerical calculations, on the model with step function solitons. We shall also neglect the back-reaction

of the fermions on the boson field, treating ϕ as an unmodified oscillating background. This is a natural approximation when the coupling g is small, and is in any case necessary when working with the signum function domain walls, whose dynamical equations would involve singular quantities.

An algorithm for integrating the Dirac equation is going to encounter difficulties at the boundaries of the integration domain, because the solutions of the unmodified Dirac equation may be dominated by convective behavior—which will typically involve energies modes propagating inward from infinity as well as outward toward infinity. This is obviously contrary to the radiation boundary conditions we would like to impose.

If the initial Dirac wave function is well localized around the soliton-containing region, then at small times, the numerical solution in the radiation zone will be dominated, as desired, by the outgoing fermion and antifermion modes. However, if the Dirac field is not subject to unphysical conditions (such as the strong spatial damping described below) at or near the ends of the integration domain, then when the outgoing excitations start to impinge on the exterior boundaries, the algorithm will suffer from an unstable explosion of unphysical incoming mode excitations. A small numerical error will introduce an admixture of incoming waves into the solution, with the error due to these spurious modes increasing with time. The field itself will begin to blow up at the boundary, and the inward propagation will rapidly wreck the calculated solution.

There might seem to be an obvious solution to the instabilities at the left and right boundaries—applying strong damping to the equation in the vicinities of the boundaries. Indeed, some of the built-in integration algorithms in Mathematica software are "clever" enough to make this suggestion. Applying such an unphysical modification to the standard Dirac equation does indeed improve the reliability of integration algorithms for a certain amount of time. However, over longer periods, this method is not satisfactory either. The problem arises from the fact that the method is similar to pegging the value of the Dirac field to zero at the ends of the integration region. As a result, over longer times, the solution eventually degrades into what is essentially a driven (by the oscillating domain walls) standing wave, rebounding back and forth between the two ends of the integration interval.

To deal with these complications, we integrated the evolution over an extended spatial domain, so that the leading edge of the outgoing pulse, moving at the signal speed $c_s = 1$, never reached the vicinity of the boundary. The resulting wave functions were then simply cropped down to the region of physical interest. Figures 1–3 show the results (plotted as the absolute values of ψ_1 and ψ_2) for coupling values $g = 0.10$, 0.25, and 0.50. The initial states used in the calculations were negative-energy bound states of the potential at time $t = 0$—the almost-zero-energy modes of $V(x, 0)$ that are symmetric combinations of the localized modes around $v = 10$ and $-v = -10$ [43].

Studying these plots, a number of significant features may be observed. The parity symmetry is clearly evident, since $\psi_1(x, t)$ and $\psi_2(x, t)$ are mirror images of each other across the line $x = 0$. (This provides an important "sanity check" of the computational results.) The diagonal lines indicating the propagation of fronts are also very obvious. The slopes of the visible lines are, as they should be, the signal velocities $\pm c_s$; the signal speed c_s is the phase velocity for the shortest-wavelength modes, which is, according to (24), simply the propagation speed of massless excitations in vacuum, $c_s = 1$.

Although initially ψ_1 is strongly localized around the kink and ψ_2 around the antikink, the time-dependence of the background causes the solution around $x_K = -v = -10$ to acquire a ψ_2 component fairly quickly. The kink and antikink in (4) start from rest, but it does not take long for their motion to couple the two wave function components together. As a result, over most of the integration time interval, ψ_1 and ψ_2 are comparable everywhere in the spatial domain. From each of the regions around $x = \pm v$ where the wave functions are initially localized, each of ψ_1 and ψ_2 shows an pattern of expansion at the speed c_s. At short times, this may look like oscillation-stimulated tunneling from the bound state to continuum states. However, the outflow from the soliton regions continues indefinitely; in particular, there continues to be outgoing radiation after the oscillation amplitude of $|\psi|^2$ in

the immediate vicinity of the domain walls has fallen to be no larger than the typical values elsewhere inside the light cone. After a time $v/c_s = 10$, the expanding cones overlap, and there is an interference region centered on $x = 0$. Interestingly, as a consequence of the way Equations (10) and (11) are coupled (with the coupling terms having explicit factors of i), the contribution to ψ_2 in the initial vicinity of ψ_1 (and vice versa) is mostly imaginary, while ψ_1 in that region remains predominantly real—at least until the expanding light cones based at $\pm v$ begin to overlap. This fact is evident from Figure 4, which shows the typical behavior of the real and imaginary parts of ψ.

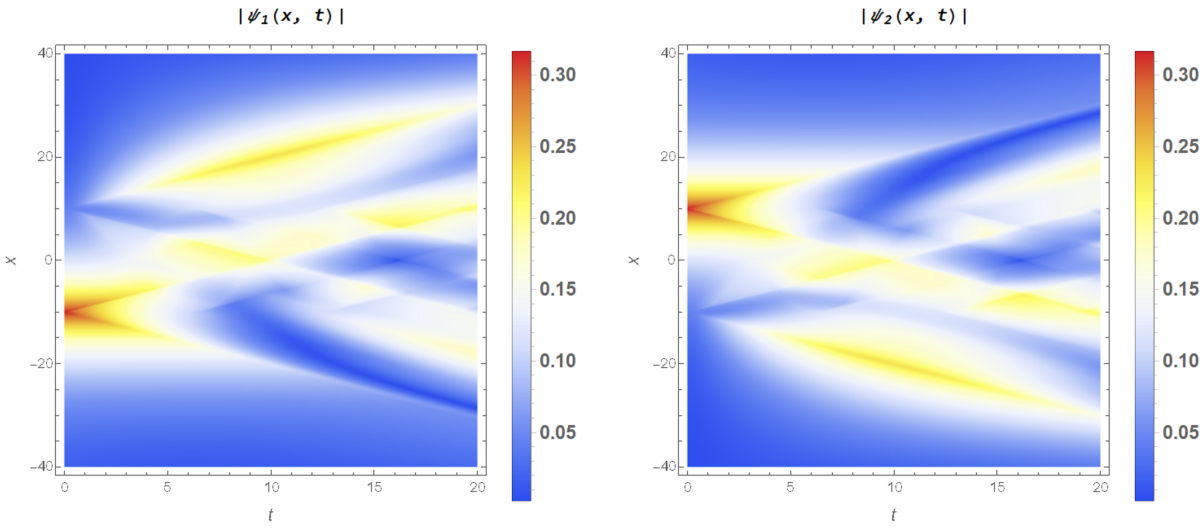

Figure 1. The upper (**left**) and lower (**right**) components of the time-evolving Dirac wave function, plotted in terms of position x and time t for the coupling value $g = 0.10$, domain wall oscillation amplitude $v = 10$, and frequency $\omega = 0.50$. The starting ψ is a symmetric bound state of the instantaneous $V(x, t = 0)$.

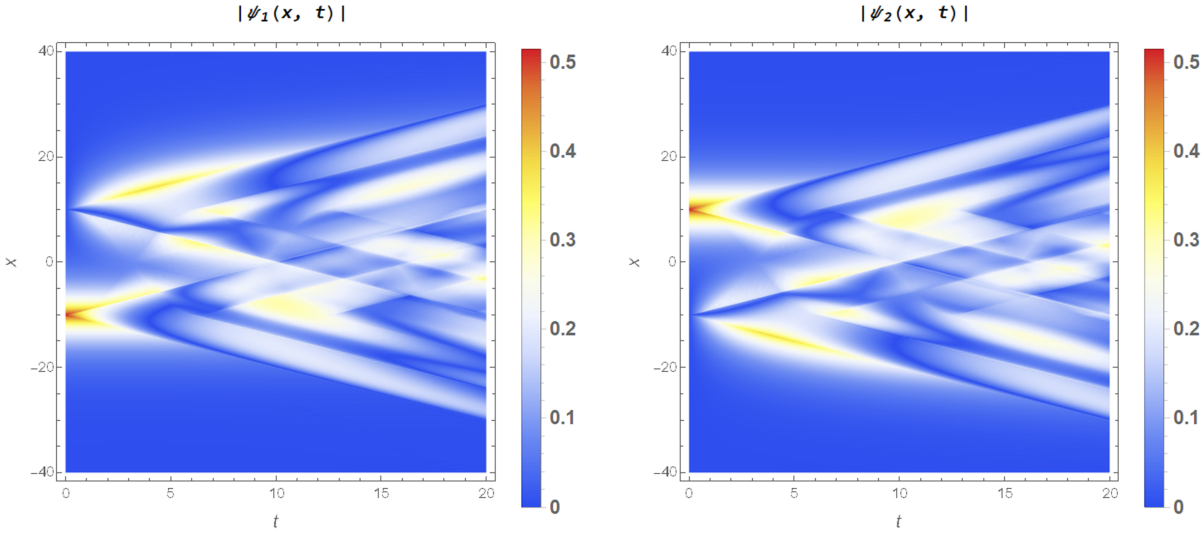

Figure 2. The upper (**left**) and lower (**right**) components of the wave function, for the coupling $g = 0.25$.

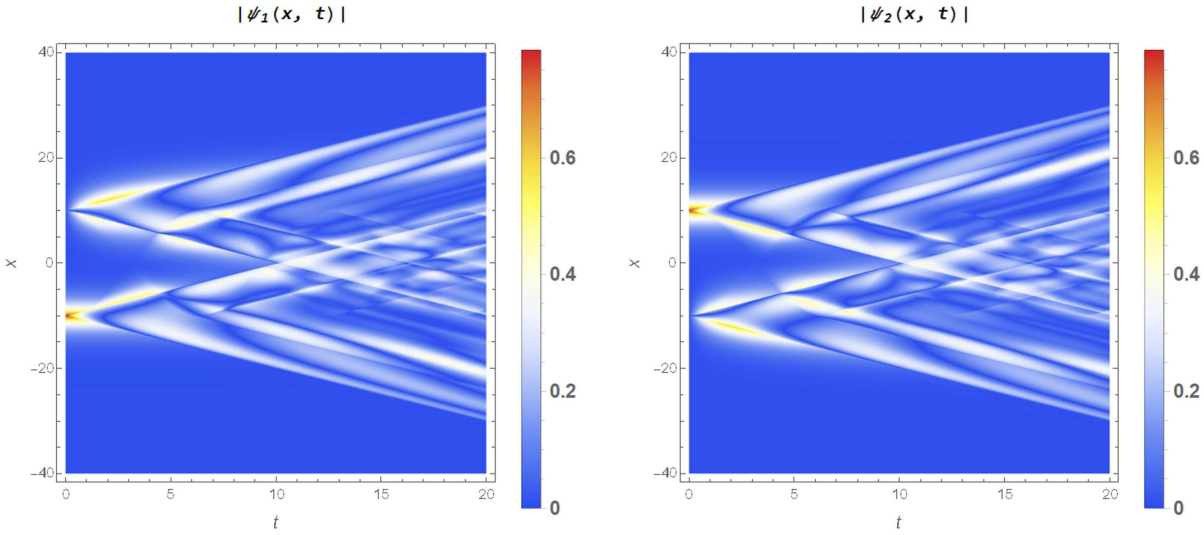

Figure 3. The upper (**left**) and lower (**right**) components of the wave function, for the coupling $g = 0.50$.

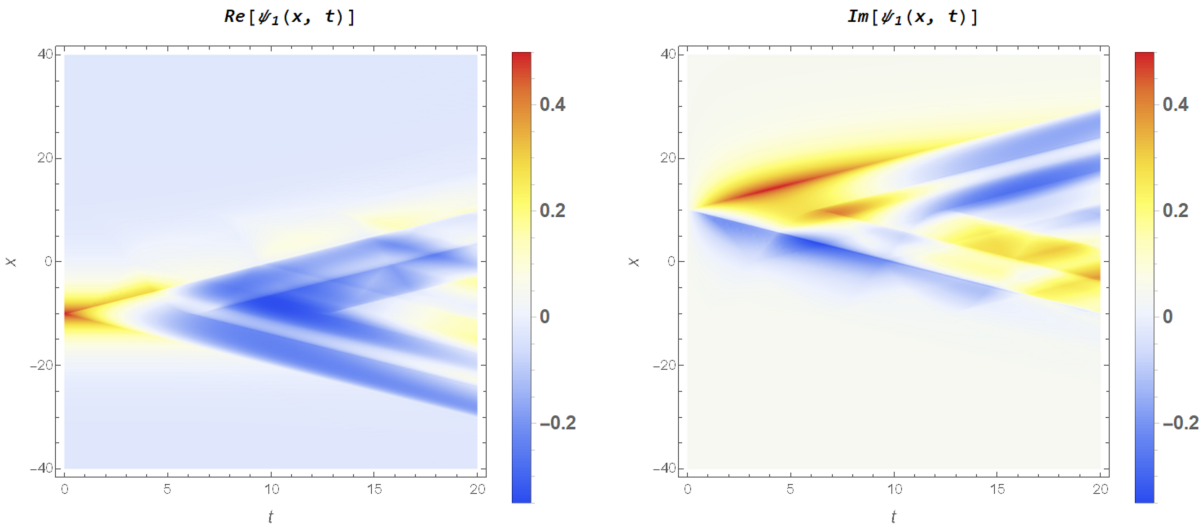

Figure 4. Real and imaginary parts of ψ_1 for $g = 0.25$.

In all the figures, but particularly in Figure 5, which shows the total $\psi^\dagger\psi = |\psi_1|^2 + |\psi_2|^2$, the oscillation period $\pi/\omega = 2.0\pi$ of the domain wall potential (5) is also visible. There are quite evidently multiple pairs of nested signal cones. Although the greatest part of the flux lies on the primary shock fronts, enough particle density remains near the initial positions at $v = \pm 10$ for there to be partial recurrences of the initial peaks after one oscillation period of the potential. These are indicated by the cusps in the plots that form the lying at t coordinate π/ω. There is another feature, of the same nature, at $t = 2\pi/\omega$, although it is markedly less pronounced, since relatively little particle density remains anywhere near $\pm v$ after that much time has passed.

The partial recurrence—and thus the nested cones that are visible to greater or lesser extents in all the figures—is actually the most visually salient feature that is specific to a situation in which the initial conditions represent a fermion wave function that is strongly peaked around one or both of the domain walls. For initial states peaked elsewhere, the general light cone expansion looks not especially dissimilar to what is shown in Figures 1–3. Within each cone, there is an additional wave structure, visible as blue and white striations in those three figures, with a wavelength that decreases with increasing g.

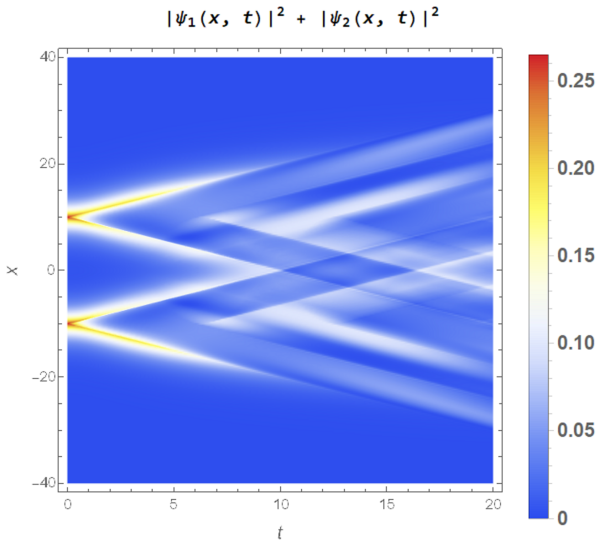

Figure 5. Total particle density $\psi^\dagger\psi$ for the solution with $g = 0.25$.

6. Conclusions

The paper has delved into the complex dynamics of fermion interactions in a time-dependent breather-like background, specifically focusing on oscillating domain walls. Our analysis shows that, despite the initial hopes for integrable behavior akin to the purely bosonic sine-Gordon theory, the fermion modes exhibit unavoidable outward flux. This flux is driven energetically by the oscillations of the scalar field, resulting in the eventual escape of fermion–antifermion pairs to infinity, as illustrated in Figures 1–3.

A key finding is that although fermion wave functions initially appear bound to the domain walls, over time, they do not remain localized, and indeed, they do not remain significantly more localized than arbitrary wave functions that are not closely approximated by bound states of the static forms of the potentials. In either case, the oscillating backgrounds lead to the propagation of fermionic states outward at speeds up to the speed of light, as demonstrated by the cone-shaped shock fronts seen in the graphs (i.e., Figure 1 for $g = 0.10$, Figure 2 for $g = 0.25$, and Figure 3 for $g = 0.50$). These graphs clearly depict the expansion of the fermionic excitations beyond the domain wall regions, showing the spread of interacting fermion wave functions across space. This is rather unlike the behavior often seen in the purely bosonic sectors of higher-order non-integrable models [44,45], in which the effective potentials between the solitary waves in $1+1$ dimensions [12,46] tend to remain well localized, even when the individual kinks and antikinks possess fat tails [13].

Numerical simulations show that even though some particle density remains localized near the initial positions of the domain walls after one oscillation period (visible as partial recurrences in Figure 5), the overall trend is a wave of flux moving toward spatial infinity. This feature underscores the limitations of approximating such systems as fully integrable, as the outward particle flux becomes a significant factor in the system's long-term behavior. Moreover, after a sharp falloff in the fermion field amplitude at small times, the oscillating fermion fields do not damp to zero at large times. Instead, their amplitudes remain finite and comparable throughout the light cone interiors, as the motion of the kink–antikink pair continues to pump energy into the fermion sector.

Further computational challenges arise due to the difficulty in imposing stable boundary conditions, particularly in light of the fermionic modes propagating outward. Attempts to impose radiation-like boundary conditions encountered confounding issues, as damping methods applied to the Dirac equation led to standing waves rebounding between the integration domain boundaries. This behavior is illustrated by the numerical instabilities at the boundaries that arise over extended integration times, as discussed in Section 5.

In addition to the outward flux of fermionic modes, our results also reveal interesting quasiperiodic behavior of the solutions, particularly around the time value of π/ω, which corresponds to half the oscillation period of the moving domain walls and one full oscillation period of potential $V(x,t)$. This periodicity is clearly reflected in the recurrence of fermion density peaks at the initial positions of the domain walls, as seen in Figures 1–5. After each oscillation cycle, the particle densities exhibit partial recurrences, although with diminishing intensity, as the fermion modes continue to propagate outward.

In Figure 5, which shows the total particle density $\psi^\dagger\psi$ for $g = 0.25$, two distinct sets of nested cones are clearly visible (and a third one less clearly). These cones reflect the periodic return of fermion density near $x = \pm v = \pm 10$, which aligns with the oscillation period π/ω. The first recurrence is quite pronounced, with the peaks in particle density forming sharp cusps around $t = \pi/\omega$, indicating that a significant portion of the fermion density remains bound near the domain walls after one period. By $t = 2\pi/\omega$, a second, less pronounced recurrence is visible, suggesting that most of the particle density has dissipated away by this time, but a small amount still remains in the vicinity of the original domain wall positions.

The oscillatory nature of the scalar potential, with period π/ω, governs this periodic recurrence. As the domain walls oscillate, they periodically couple and decouple the fermion wave functions, leading to these recurrences of fermion densities after each full oscillation cycle. However, over time, the amplitude of these recurrences decreases as more fermion density escapes toward spatial infinity. This feature, seen in the graphs, underscores the non-adiabatic nature of the system, where the periodic motion of the domain walls continuously injects energy into the fermionic modes, driving particle production and flux.

Overall, this analysis concludes that the sine-Gordon-like breather background, when coupled to fermions, does not generally support steady-state bound fermion solutions. Instead, the oscillations induce fermion particle production and flux propagation, suggesting that the fermion–soliton system does not maintain the integrability and stability expected from the purely bosonic sine-Gordon theory. It may be possible in the future to test these theoretical results in real systems with topological configurations of boson fields coupled to fermionic particles.

Author Contributions: Conceptualization, B.A.; methodology, B.A. and A.R.; software, B.A. and A.R.; validation, B.A. and A.R.; formal analysis, B.A. and A.R.; investigation, B.A. and A.R.; resources, B.A.; data curation, B.A. and A.R.; writing—original draft preparation, B.A. and A.R.; writing—review and editing, B.A. and A.R.; visualization, B.A. and A.R.; supervision, B.A.; project administration, B.A. All authors have read and agreed to the published version of the manuscript.

Funding: This research received no external funding.

Data Availability Statement: Data are contained within the article.

Acknowledgments: The authors thank S. Crittenden for software assistance.

Conflicts of Interest: The authors declare no conflicts of interest.

References

1. Unruh, W.G. Notes on black-hole evaporation. *Phys. Rev. D* **1976**, *14*, 870. [CrossRef]
2. Hawking, S.W. Particle creation by black holes. *Commun. Math. Phys.* **1975**, *43*, 199. [CrossRef]
3. Jackiw, R.; Rebbi, C. Solitons with fermion number 1/2. *Phys. Rev. D* **1976**, *13*, 3398. [CrossRef]
4. Campbell, D.K.; Schonfeld, J.F.; Wingate, C.A. Resonance structure in kink-antikink interactions in ϕ^4 theory. *Phys. D Nonlin. Phenom.* **1983**, *9*, 1. [CrossRef]
5. Riazi, N.; Azizi, A.; Zebarjad, S.M. Soliton decay in a coupled system of scalar fields. *Phys. Rev. D* **2002**, *66*, 065003. [CrossRef]
6. Mansouri, K.; Riazi, N. Dynamics of solitons in coupled system of scalar fields. *Int. J. Theor. Phys.* **2005**, *44*, 309. [CrossRef]
7. Bazeia, D.; Mohammadi, A.; Moreira, D.C. Fermion bound states in geometrically deformed backgrounds. *Chin. Phys. C* **2019**, *43*, 013101. [CrossRef]
8. Izquierdo, A.A.; Queiroga-Nunes, J.; Nieto, L.M. Scattering between wobbling kinks. *Phys. Rev. D* **2021**, *103*, 045003. [CrossRef]

9. Navarro-Obregón, S.; Nieto, L.M.; Queiruga, J.M. Inclusion of radiation in the collective coordinate method approach of the ϕ^4 model. *Phys. Rev. E* **2023**, *108*, 044216. [CrossRef]
10. Manton, N.S. An effective Lagrangian for solitons. *Nucl. Phys. B* **1979**, *150*, 397. [CrossRef]
11. González, J.A.; Estrada-Sarlabous, J. Kinks in systems with degenerate critical points. *Phys. Lett. A* **1989**, *140*, 189. [CrossRef]
12. Christov, I.C.; Decker, R.J.; Demirkaya, A.; Gani, V.A.; Kevrekidis, P.G.; Khare, A.; Saxena, A. Kink-kink and kink-antikink interactions with long-range tails. *Phys. Rev. Lett.* **2019**, *122*, 171601. [CrossRef] [PubMed]
13. Christov, I.C.; Decker, R.J.; Demirkaya, A.; Gani, V.A.; Kevrekidis, P.G.; Radomskiy, R.V. Long-range interactions of kinks. *Phys. Rev. D* **2019**, *99*, 016010. [CrossRef]
14. Manton, N.S. Integration theory for kinks and sphalerons in one dimension. *J. Phys. A Math. Theor.* **2023**, *57*, 025202. [CrossRef]
15. Manton, N.S. Antikink-kink forces revisited. *arXiv* **2024**, arXiv:2410.15412.
16. Sugiyama, T. Kink-antikink collisions in the two-dimensional ϕ^4 model. *Prog. Theor. Phys.* **1979**, *61*, 1550. [CrossRef]
17. Anninos, P.; Oliveira, S.; Matzner, R.A. Fractal structure in the scalar $\lambda(\phi^2-1)^2$ theory. *Phys. Rev. D* **1991**, *44*, 1147. [CrossRef]
18. Goodman, R.H.; Haberman, R. Kink-antikink collisions in the ϕ^4 equation: The n-bounce resonance and the separatrix map. *SIAM J. Appl. Dyn. Syst.* **2005**, *4*, 1195. [CrossRef]
19. Belendryasova, E.; Gani, V.A. Scattering of the ϕ^8 kinks with power-law asymptotics. *Comm. Nonlin. Sci. Numer. Sim.* **2019**, *67*, 414. [CrossRef]
20. Belendryasova, E.; Gani, V.A.; Zloshchastiev, K.G. Kink solutions in logarithmic scalar field theory: Excitation spectra, scattering, and decay of bions. *Phys. Lett. B* **2021**, *83*, 136776. [CrossRef]
21. Izquierdo, A.A.; Nieto, L.M.; Queiroga-Nunes, J. Asymmetric scattering between kinks and wobblers. *Comm. Nonlin. Sci. Numer. Sim.* **2022**, *107*, 106183. [CrossRef]
22. Su, W.P.; Schrieffer, J.R. Fractionally charged excitations in charge-density-wave systems with commensurability 3. *Phys. Rev. Lett.* **1981**, *46*, 738. [CrossRef]
23. Kivelson, S.; Schrieffer, J.R. Fractional charge, a sharp quantum observable. *Phys. Rev. B* **1982**, *25*, 6447. [CrossRef]
24. Frishman, Y.; Horovitz, B. Charge fluctuations and fractional charge of fermions in $1+1$ dimensions. *Phys. Rev. B* **1983**, *27*, 2565. [CrossRef]
25. Hirata, Y.; Minakata, H. Soliton-antisoliton pair creation in strong external fields. *Phys. Rev. D* **1987**, *36*, 652(R). [CrossRef]
26. Karki, S.; Altschul, B. Creation of bound half-fermion pairs by solitons. *Eur. Phys. J. C* **2024**, *84*, 397. [CrossRef]
27. Wazwaz, A.-M. Multiple kink solutions for two coupled integrable $(2+1)$-dimensional systems. *Appl. Math. Lett.* **2016**, *58*, 1. [CrossRef]
28. Ma, W.-X. N-soliton solution and the Hirota condition of a $(2+1)$-dimensional combined equation. *Math. Comp. Sim.* **2021**, *190*, 270. [CrossRef]
29. Gao, X.-Y. Auto-Bäcklund transformation with the solitons and similarity reductions for a generalized bonlinear shallow water wave equation. *Qual. Theor. Dyn. Syst.* **2024**, *23*, 181. [CrossRef]
30. Gao, X.-Y. Symbolic computation on a $(2+1)$-dimensional generalized nonlinear evolution system in fluid dynamics, plasma physics, nonlinear optics and quantum mechanics. *Qual. Theor. Dyn. Syst.* **2024**, *23*, 202. [CrossRef]
31. Rajaraman, R. *Solitons and Instantons*; Elsevier: Amsterdam, The Netherlands, 1982; pp. 291–298.
32. Shifman, M.; Vainshtein, A.; Voloshin, M. Anomaly and quantum corrections to solitons in two-dimensional theories with minimal supersymmetry. *Phys. Rev. D* **1999**, *59*, 045016. [CrossRef]
33. Chu, Y.-Z.; Vachaspati, T. Fermions on one or fewer kinks. *Phys. Rev. D* **2008**, *77*, 025006. [CrossRef]
34. Amado, A.; Mohammadi, A. Coupled fermion–kink system in Jackiw–Rebbi model. *Eur. Phys. J. C* **2017**, *77*, 465. [CrossRef]
35. Graham, N.; Jaffe, R.L. Fermionic one-loop corrections to soliton energies in $1+1$ dimensions. *Nucl. Phys. B* **1999**, *549*, 516. [CrossRef]
36. Goldhaber, A.S.; Litvintsev, A.; van Nieuwenhuizen, P. Mode regularization of the supersymmetric sphaleron and kink: Zero modes and discrete gauge symmetry. *Phys. Rev. D* **2001**, *64*, 045013. [CrossRef]
37. Brihaye, Y.; Delsate, T. Remarks on bell-shaped lumps: Stability and fermionic modes. *Phys. Rev. D* **2008**, *78*, 025014. [CrossRef]
38. Perapechka, I.; Shnir, Y. Kinks bounded by fermions. *Phys. Rev. D* **2020**, *101*, 021701(R). [CrossRef]
39. Ferrara, S.; Girardello, L.; Sciuto, S. An infinite set of conservation laws of the supersymmetric sine-Gordon theory. *Phys. Lett. B* **1978**, *76*, 303. [CrossRef]
40. Bajnok, Z.; Dunning, C.; Palla, L.; Takács, G.; Wágner, F. SUSY sine-Gordon theory as a perturbed conformal field theory and finite size effects. *Nucl. Phys. B* **2004**, *679*, 521. [CrossRef]
41. Klein, O. Die Reflexion von Elektronen an einem Potentialsprung nach der relativistischen Dynamik von Dirac. *Z. Physik* **1929**, *53*, 157. [CrossRef]
42. Sauter, F. On the behavior of an electron in a homogeneous electric field in Dirac's relativistic theory. *Z. Phys.* **1931**, *69*, 742. [CrossRef]
43. Scott, T.C.; Babb, J.F.; Dalgarno, A.; Morgan, J.D. The calculation of exchange forces: General results and specific models. *J. Chem. Phys.* **1993**, *99*, 2841. [CrossRef]
44. Khare, A.; Christov, I.C.; Saxena, A. Successive phase transitions and kink solutions in ϕ^8, ϕ^{10}, and ϕ^{12} field theories. *Phys. Rev. E* **2014**, *90*, 023208. [CrossRef] [PubMed]

45. Bazeia, D.; Menezes, R.; Moreira, D.C. Analytical study of kinklike structures with polynomial tails. *J. Phys. Comm.* **2018**, *2*, 055019. [CrossRef]
46. Mello, B.A.; González, J.A.; Guerrero, L.E.; López-Atencio, E. Topological defects with long-range interactions. *Phys. Lett. A* **1998**, *44*, 277. [CrossRef]